W-band waveguide filter based on large TM120 resonators to ease CNC milling

Shang, Xiaobang; Lancaster, Michael; Dong, Yu-Liang

DOI:
10.1049/el.2016.4131

W-band waveguide filter based on large TM120 resonators to ease CNC milling

Xiaobang Shang, M. J. Lancaster and Yu-Liang Dong

A W-band waveguide bandpass filter, based on coupled TM_{120} resonators, fabricated using CNC milling, is presented. TM_{120} resonators are superior to conventional TE_{101} resonators, in terms of having a larger size and reduced aspect ratio, which facilitates the fabrication process as well as allowing larger tolerances in the milling process. This type of resonator also offers a high unloaded quality factor, and ultimately yields a small insertion loss for the filter. A W-band filter, with a center frequency of 100 GHz and a fractional bandwidth (*FBW*) of 6%, is designed using four TM_{120} resonators and constructed from three brass shims which directly fit to the waveguide flanges. This filter is measured to have a median passband insertion loss of 0.5 dB and a return loss better than 13 dB across the whole passband.

Introduction: Waveguide filters are essential components used in many microwave systems. Traditionally, computer numerical control (CNC) milling is widely used to machine high frequency waveguide devices from metal. When frequencies rise above W-band and beyond, it becomes more and more challenging to produce waveguide devices using conventional CNC milling due to the reduction in size and tight tolerances demanded by such waveguides. Researchers have been actively exploring alternative manufacturing techniques to cope with the increasing requirements on dimensional accuracy and surface quality. High frequency waveguide devices with good measurement performance have been demonstrated by 3-D printing (e.g. [1]), laser micromachining [1], silicon deep reactive ion etching (DRIE) (e.g. [2]), and thick SU-8 process (e.g. [3]). The latter two approaches are based on lithography technology and are therefore capable of patterning small features accurately. Currently however, they require the use of a relatively expensive cleanroom as well as an additional metal coating process, which makes them cost-effective only for large scale production.

Waveguide devices milled directly from metal are still preferred for applications involving high operating temperatures, demanding a good thermal stability and durability, and for small to medium size batch production. Examples of waveguide filters made on state-of-the-art expensive CNC machines are reported in W-band [4] and WR-3 band [5]. All of these filters utilize the conventional TE_{101} resonators and symmetrical inductive coupling irises.

In this work, we propose the use of TM_{120} resonators for construction of high frequency waveguide filters using CNC milling. Such resonators ease the CNC milling process in terms of having a larger size as well as a reduced aspect ratio, in comparison with standard TE_{101} resonators, without sacrificing unloaded quality factor (Q_u). In addition, filters made by TM_{120} resonators permit a less stringent tolerance, and this could yield a significant reduction in cost. At low frequencies (~10 GHz), dual-mode resonators operating at both TM_{120} and TM_{210} modes have been utilized to implement advanced waveguide filters with minimized size and/or transmission zeros (e.g. [6]). Here, we focus on exciting a single mode and attempting to make use of the TM_{120} resonators' large size. A W-band filter based on four coupled TM_{120} resonators as shown in Fig. 1, is designed and presented.

TM_{120} Resonators: Fig. 2*a* is an illustration of a TM_{120} resonator. Usually, TM mode cavities are used in a dual mode configuration, i.e. TM_{120} mode and TM_{210} mode [6]. Resonant frequencies of both of these two modes depend upon *w* and *h* only. In the case where *w*=*h*, TM_{120} and TM_{210} have the same resonant frequency. The excitation of TM_{210} mode can be avoided as a result of the way the coupling irises are placed, as discussed in the following section. Table 1 presents a comparison between a TM_{120} resonator and a conventional TE_{101} resonator. It is found that the TM_{120} resonator is almost twice as large as the TE_{101} resonator. The TM_{120} resonator has a lower aspect ratio (~1: 0.3) in contrast with that of TE_{101} resonator (~1: 0.7). Here the aspect ratio is the ratio of the resonators' smallest width to height (i.e. *w: l* for the TM_{120} resonator). For W-band and terahertz waveguide filters, a lower aspect ratio is always desired as it eases the fabrication and metal coating (if required), and leads to a better surface integrity at sidewalls. Both resonators are simulated in CST Microwave Studio, and their calculated unloaded quality factors, Q_u, are given in Table 1. An even higher Q_u than the one in Table 1 is achievable for a TM_{120} resonator by increasing *l*. On the other hand, an increase in *l* brings down the resonant frequencies of the spurious TE_{101} and TE_{011} modes, which could have degraded the filter's performance over the higher out-of-band frequencies. Fig. 2*b* shows the calculated frequency shift due to small errors in dimensions for TM_{120} and TE_{101} resonators. Larger volume TM_{120} resonators reduce their sensitivity to dimensional inaccuracies, however, this is at the cost of having a larger family of spurious modes. Among them, the most significant two are TM_{110} (occurring at 63 GHz) and TM_{220} (resonating at 127 GHz), which are fairly close to the lower and upper limit of W-band. However, their impact on the far out-of-band responses can be minimized/eliminated, since it is feasible to prevent the excitation and propagation of these modes by controlling how the resonator is coupled, as described in the section below.

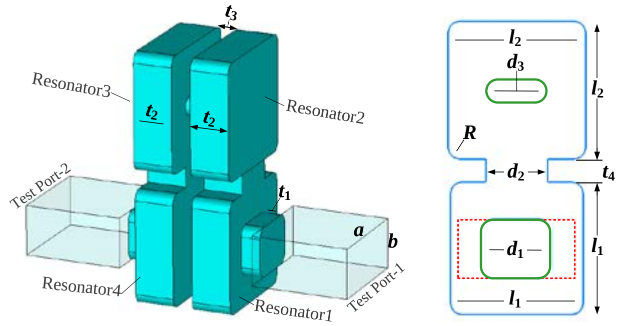

a *b*

Fig. 1 *Illustration diagrams of the W-band filter based on four coupled TM_{120} resonators.*
a Configuration of the filter structure with test input and output. Input/output waveguides are not part of the filter. *a*=2.54, *b*=1.27, t_1=0.5, t_2=1, t_3=0.5.
b Schematic front view diagram of the filter. The red rectangular (in dashed lines) indicates the input/output waveguide of the test equipment, whereas the green rounded rectangles represent for coupling irises which are employed to provide external coupling as well as coupling between resonators 2 and 3. l_1=2.889, l_2=3.001, d_1=1.509, d_2=1.354, d_3=1.309, t_4=0.5, *R*=0.25. Unit: millimeter.

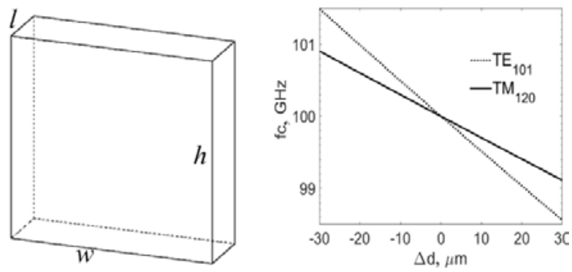

a *b*

Fig. 2 *Diagram of a TM_{120} resonator and calculated resonant frequencies (fc) of TM_{120} and TE_{101} resonators as a function of dimensional error Δd (assumed to be the same on three axes).*
a Configuration of a TM_{120} resonator.
b Calculated resonant frequency shift due to errors in dimensions, for a TE_{101} and a TM_{120} resonator.

Table 1: Comparison between TE_{101} resonator and TM_{120} resonator with the same resonant frequency of 100 GHz.

Resonator	TM_{120}	TE_{101}
Size (mm)	3.352×3.352×1	2.54×1.27×1.857
Volume (mm^3)	11.235	5.990
Q_u	2060	1865
First spurious higher mode	TM_{220} (127 GHz)	TM_{110} (132 GHz)

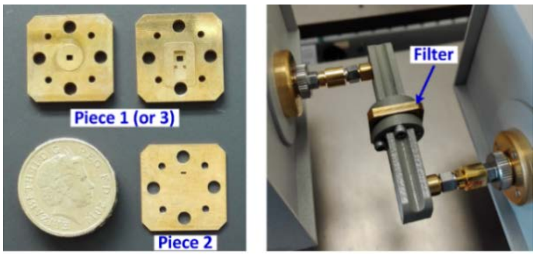

a *b*

Fig. 3 *Photograph of the W-band filter and the measurement setup.*
a Photograph of the filter. Pieces 1 and 3 are identical.
b Photograph of the measurement setup.

Filter Design and Fabrication: A fourth-order W-band filter centered at 100 GHz with a fractional bandwidth (*FBW*) of 6% has been designed using TM_{120} resonators. This filter is designed to have a Chebyshev response with a passband return loss of 20 dB. Based on these specifications, the external quality factors and the non-zero coupling coefficients are calculated to be [7] $Q_{ext} = 15.5233$, $k_{12} = k_{34} = 0.0547$ and $k_{23} = 0.042$. These coupling coefficients can be converted to physical dimensions by following the procedure given in [7]. The filter structure is shown in Fig. 1. As shown in Fig. 1*a*, the external couplings are realized through an iris which is coupled to the center of resonator 1 (or 4). This arrangement ensures that the magnetic fields of the TM_{210} and TM_{110} modes are perpendicular to that of the feeding waveguide, and therefore neither of these two unwanted modes can be excited [6]. Such an arrangement ensures the filter operates at the single mode and has a clear lower stopband (TM_{110} is the only spurious mode below 100 GHz). For the same reason, the coupling iris between resonators 2 and 3 is also placed in the centre. It can be observed from above discussions that the prevention of unwanted modes depends greatly on the symmetry of the structure. This imposes additional requirements on the fabrication and assembling.

Full-wave modeling for this filter is carried out using CST. Fig. 1*b* exhibits detailed dimensions of this filter, and Fig. 4 shows the corresponding simulation results. Note that, the conductivity of brass, 2.74×10^{7} S/m, is employed in the simulations, as well as the calculations of Q_u presented in Table 1.

The filter is machined from brass on a standard CNC machine. Three brass shims form the filter, as shown in Fig. 3*a*. The areas around the functional contact surfaces stand out by 100 μm, to prevent them from hindering the proper contact between the functional areas. This effort to minimize the contact area is made to deal with imperfect flatness of brass shims. Additionally, brass is chosen in this work due to its good machinability. In the scenario where a minimized insertion loss is desired, the filter could be either coated with a thin gold layer or machined directly from copper.

Measurement and Results: Measurement is carried out using an Agilent N5250A network analyzer subject to a TRL (thru-reflect-line) calibration. During the measurements, the three brass shims of the filter are sandwiched between the flanges of the network analyzer measurement heads, as shown in Fig. 3*b*. Four flange pins are employed to align the three shims, as well as to align the filter to the flanges, whereas screws attached to the flanges are utilized to provide a good contact between them. Fig. 4 shows the measurement results (over the whole W-band) which agree well with the simulations. There is no tuning of the filter, and no smoothing or averaging is performed on the measured results.

The measured passband insertion loss and the return loss is 0.5 dB and better than 13 dB, respectively. The measured insertion loss is 0.2 dB higher than the value obtained from CST simulations using the conductivity of brass. This small extra loss is mainly attributed to (i) leakage between layers; and (ii) surface roughness (introduced during milling process) which degrades the effective conductivity of brass. The worsen-than-simulated S_{11} is believed to be due to (i) misalignments between layers of the filter and/or between the filter and the flanges; and (ii) small dimensional inaccuracies for some features which are measured to be within 10 μm.

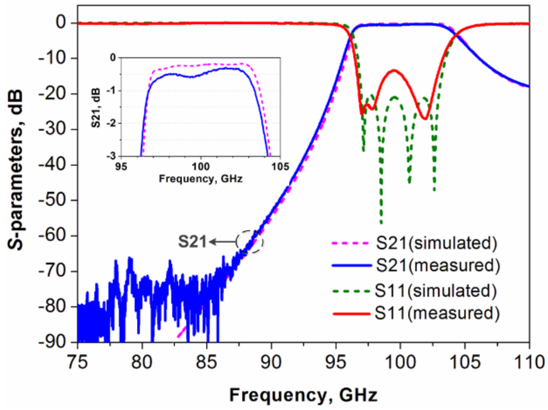

Fig. 4 *Measurement (solid lines) and simulation (dashed lines) results of the W-band filter. The insert shows an enlarged view of the S_{21} responses over the passband.*

Conclusion: A W-band filter based on TM_{120} resonators has been reported. This filter is the first-ever demonstrated high frequency waveguide filter based on TM_{120} resonators. This type of filter facilitates CNC machining and relaxes the requirement on tight tolerances. A very good agreement between the measurement and simulation results of the filter is achieved. The proposed filter structure may find useful applications in the design of terahertz waveguide filters which usually require designs less sensitive to fabrication inaccuracies.

Acknowledgments: This work was supported by the U.K. Engineering and Physical Science Research Council (grant EP/M016269/1).

X. Shang and M. J. Lancaster (*Department of Electronic Electrical and Systems Engineering, The University of Birmingham, Birmingham, United Kingdom*)

E-mail: x.shang@bham.ac.uk

Y. L. Dong (*National Institute of Measurement and Testing Technology, 10 Yushuang Road, Chenghua District, Chengdu 610021, People's Republic of China*)

References

1. Shang, X., Penchev, P., Guo, C., Lancaster, M. J., Dimov, S., Dong, Y. L., Favre, M., Billod, M., and Rijk, E.: 'W-band waveguide filters fabricated by laser micromachining and 3-D printing', *IEEE Trans. Microw. Theory Techn.*, 2016, **64**, (8), pp. 2572–2580, doi: 10. 1109/ TMTT.2016.2574839
2. Leal-Sevillano, C.A., Reck, T. J., Jung-Kubiak, C., Chattopadhyay, G., Ruiz-Cruz, J. A., Montejo-Garai, J. R., and Rebollar J. M.: 'Silicon micromachined canonical E-plane and H-plane bandpass filters at the terahertz band', *IEEE Microw. Wirel. Compon. Lett.*, 2013, **23**, (6), pp. 288–290, doi: 10.1109/LMWC.2013.2258097
3. Shang, X., Ke, M. L., Wang, Y., and Lancaster, M. J.: 'Micromachined WR-3 waveguide filter with embedded bends', *Electronics Lett.*, 2011, **47**, (9), pp. 545–547, doi: 10.1049/el.2011.0525
4. Leal-Sevillano, C. A., Montejo-Garai, J. R., Ruiz-Cruz, J. A., and Rebollar, J. M. : 'Low-loss elliptical response filter at 100 GHz', *IEEE Microw. Wirel. Compon. Lett.*, 2012, **22**, (9), pp. 459–461, doi: 10.1109 / LMWC .2012 .2212237
5. Zhuang, J. X., Hong, W., and Hao, Z. C.: 'Design and analysis of a terahertz bandpass filter', IEEE International Wireless Symposium (IWS), Shenzhen, China, March 2015, pp.1–4, doi: 0.1109/IEEE-IWS. 2015.7164597
6. Tomassoni, C., Bastioli, S., and Sorrentino, R.: 'Generalized TM dual-mode cavity filters', *IEEE Trans. Microw. Theory Technol.*, 2011, **59**, (12), pp. 3338−3346, doi: 10.1109/TMTT.2011.2172622
7. Hong, J., and Lancaster, M. J.: 'Microstrip filters for RF/microwave applications' (John Wiley & Sons, Inc., New York, 2004, 1st edition)